

Alkyl Chain Length Effects on Double-Deck Assembly at the Liquid/Solid Interface

Yuan Fang,^[a,d] Mihaela Cibian,^[c] Garry S. Hanan,^[c] Dmitrii F. Perepichka,^[d] Steven De Feyter,^[b] Louis A. Cuccia,*^[a] Oleksandr Ivashenko*^[b]

[a] Department of Chemistry and Biochemistry, Concordia University, 7141 Sherbrooke St. W., Montreal, QC, H4B 1R6, Canada.

[b] Department of Chemistry, KU Leuven, Division of Molecular Imaging and Photonics, Laboratory of Photochemistry and Spectroscopy, Celestijnenlaan 200F, 3001.

[c] Department of Chemistry, University of Montreal, 2900 Edouard-Montpetit, Montreal, Quebec H3T-1J4, Canada.

[d] Department of Chemistry, McGill University, 801 Sherbrooke Street West, Montreal, Quebec H3A 0B8, Canada.

* Corresponding authors: louis.cuccia@concordia.ca, oleksandr.ivashenko@kuleuven.be

Table of Contents

Section 1. Chemical and instrumentation.....	3
Section 2. Synthesis and characterization.....	4
Section 3. Double deck packing at chemisorbed interfaces.....	6
Figure S1. Symmetry axes of graphite	7
Figure S2. MM optimized C18m	8
Figure S3. Evidence for parallel double layer formation	8
Section 4: How to calibrate an STM image using WSxM 5.0	9

Section 1. Chemical and Instrumentation:

Chemicals 4,6-Diaminoresorcinol dihydrochloride, dodecylamine, tetradecylamine, hexadecylamine, octadecylamine, bromodocosane, hexadecyltrimethylammonium bromide, deuterated chloroform, and 1,2,4-trichlorobenzene were obtained from Aldrich. 1,4-benzoquinone was obtained from American Chemicals. Chloroform, ethyl acetate, ethanol, hexanes and methanol were obtained from Fisher Scientific. Toluene was obtained from J.T. Baker. Nickel(II) acetate tetrahydrate ($\text{Ni}(\text{OAc})_2 \cdot 4\text{H}_2\text{O}$) was obtained from BDH Chemicals. Melting points (m.p.) were recorded with a capillary melting point apparatus (Thomas Hoover). The recorded R_f values were determined by a standard thin-layer chromatography (TLC) procedure: 0.25 mm silica gel plates (Aldrich, 122785-25EA) eluted with chloroform/methanol (98:2).

NMR ^1H NMR (300 MHz) and ^{13}C NMR (75 MHz) spectra were recorded on a Varian 300 MHz spectrometer for 1-azidodocosane and docosan-1-amine at ambient temperature. ^1H NMR (500 MHz) and ^{13}C NMR (125 MHz) spectra were recorded on a Varian 500 spectrometer at ambient temperature for **C12m**, **C14m**, **C16m**, **C18m**, **C22m** and **C18p** or 45 °C for **(C18m)₂Ni**. The residual proton signals of the deuterated solvents were used as internal standards (CDCl_3 : δ (^1H) 7.26 ppm, δ (^{13}C) 77.23 ppm; the following notation is used for the ^1H NMR splitting patterns: singlet (s), doublet (d), triplet (t), quartet (q), multiplet (m) and broad signal (br).

MS For compounds **C12m**, **C14m**, **C16m**, **C18m** and **C18p**, mass spectrometric analysis was performed using a Waters Micromass, Quattro LC triple quadrupole mass spectrometer (Waters, Montreal, PQ, Canada). The instrument was operated using an ESI (electrospray ionization) source by direct injection with a syringe pump (50 μL syringe; flow rate: 1 $\mu\text{L}/\text{min}$). The MS instrument was operated in the positive mode (ES+) and the data acquisition/analysis was carried out using Masslynx software version 4.01. Source working conditions were as follows: cone voltage: 20 V, Capillary voltage: 3.3 V, source temperature: 90 °C, desolvation temperature: 100 °C, desolvation gas flow rate: 220 L/hr, nitrogen: (99.9% purity, from cylinder). Mass spectrometric analysis of each compound: 1 mg of sample was dissolved in chloroform/ethanol (1:1; 100 mL). Prior to MS analysis, 1 mL of this solution was further diluted into acetonitrile/water (1:1; 10 mL).

For compounds **C22NH₂** and **C22m**, low resolution mass measurements were performed on a LC-MSD-Tof instrument from Agilent Technologies in positive electrospray. Aliquots of 0.1

uL were injected into the mass spectrometer using a 0.5 mL/min flow of 75% methanol/ 25% water mixture. The capillary voltage was set at 3000 V and mass spectra were acquired from 100 to 1000 m/z. Both the protonated molecular ions $[M+H]^+$ and the sodium adduct $[M+Na]^+$ were used for empirical formula confirmation.

For **(C18m)₂Ni**, mass measurements were performed on Bruker Ultraflex MALDI TOF/TOF Mass Spectrometer. MALDI was used as ionization method, with dithranol as matrix, in reflector mode. The protonated molecular ion $[M]^+$ was used for empirical formula confirmation.

Section 2. Synthesis and characterization:

The detailed synthesis procedure of (a-d) can be found elsewhere.^[1]

- a) 4,6-di(dodecylamino)-*m*-quinone (**C12m**)
- b) 4,6-di(octadecylamino)-*m*-quinone (**C18m**)
- c) 2,5-di(octadecylamino)1,4-quinone (**C18p**)
- d) Bis[4-(octadecylamino)-2-(octadecylimino)-5-oxo-1,4-cyclohexadienolato]nickel (**(C18m)₂Ni**)

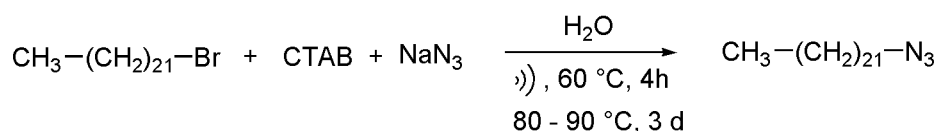
- e) (**C14m**): 4,6-Diaminoresorcinol dihydrochloride (41.2 mg; 0.193 mmol) was dispersed in ethanol (5 mL) with stirring. Tetradecylamine (336.8 mg; 1.578 mmol) was added to the stirred solution. The mixture was left to stir for *ca.* one day. The resulting dark green precipitate was isolated by vacuum filtration, washed with water and ethanol and vacuum dried. The crude product was dissolved in a minimum amount of chloroform, insoluble solids were filtered out and the filtrate was purified by centrifugal thin-layer chromatography on silica using 96:4 chloroform:methanol as eluent (69.1 mg; 0.130 mmol; 67.4%). ¹H NMR (500 MHz, CDCl₃) δ 0.90 (t, ³J = 7.0 Hz, 6H, CH₃), 1.36 (m, 44H, CH₂-CH₂-CH₂), 1.76 (p, ³J = 7.5 Hz, 4H, NH-CH₂-CH₂), 3.38 (dt, ³J = 7 Hz, 4H, NH-CH₂), 5.15 (s, 1H, NH-C-CH), 5.49 (s, 1H, O-C-CH), 8.23 (br s, 2H, NH); ¹³C NMR (125 MHz, CDCl₃): δ 14.15 (CH₃), 22.71, 26.95, 28.34, 29.18, 29.39, 29.45, 29.57, 29.64, 29.67, 29.71, 31.95, 43.32, 80.51 (N-C-C), 98.79 (O-C-C), 156.71 (N-C), 172.27 (O-C); MS (Triple Quad-ESI): m/z: 531.527 $[M+H]^+$ calcd $[M+H]^+$: 531.488.

- f) (**C16m**): 4,6-Diaminoresorcinol dihydrochloride (110.0 mg; 0.516 mmol) was dispersed in ethanol (10 mL) with stirring. Hexadecylamine (0.9145 g; 3.787 mmol) was added to the stirred solution. The mixture was heated under reflux in a water bath (controlled at 70 °C) for 2 hours. The resulting dark green precipitate was isolated by vacuum filtration (filter paper), washed

with cold ethanol and vacuum dried. The crude product was dissolved in a minimum amount of chloroform, insoluble solids were filtered out and the filtrate was purified by centrifugal thin-layer chromatography on silica using 96:4 chloroform:methanol as eluent (195.7 mg; 0.333 mmol; 64.6%). ¹H NMR (500 MHz, CDCl₃) δ 0.90 (t, ³J = 7.0 Hz, 6H, CH₃), 1.38 (m, 52H, CH₂-CH₂-CH₂), 1.76 (p, ³J = 7.5 Hz, 4H, NH-CH₂-CH₂), 3.38 (dt, ³J = 7 Hz, 4H, NH-CH₂), 5.15 (s, 1H, NH-C-CH), 5.49 (s, 1H, O-C-CH), 8.23 (br s, 2H, NH); ¹³C NMR (125 MHz, CDCl₃): δ 14.15 (CH₃), 22.72, 26.96, 28.36, 29.19, 29.39, 29.45, 29.57, 29.65, 29.69, 29.72, 31.96, 43.32, 80.52 (N-C-C), 98.79 (O-C-C), 156.71 (N-C), 172.27 (O-C); MS (Triple Quad-ESI): m/z: 587.576 [M+H]⁺ calcd [M+H]⁺: 587.551.

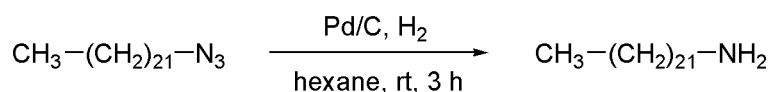
g) 4,6-di(docosylamino)-*m*-quinone (C22*m*)

1-azidodocosane:³



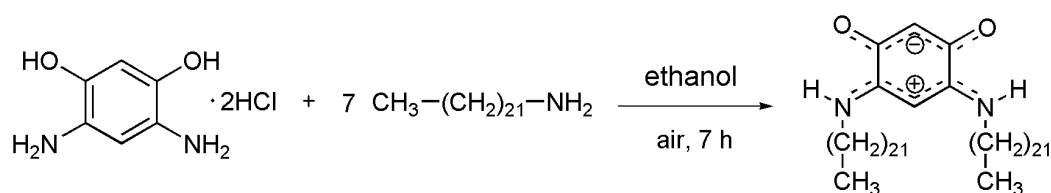
A mixture of bromodocosane (5.17 g, 13.3 mmol), hexadecyltrimethylammonium bromide (0.48 g, 1.32 mmol), sodium azide NaN₃ (2.21 g, 34.0 mmol), and water (6 mL), was sonicated at 60 °C for 4 h. The resulting slurry was refluxed (80 - 90 °C) for 3 days. Hexane was used to extract the product from the milky reaction mixture and the solid was subjected to continuous Soxhlet extraction with hexane for 1 day. The filtrate was concentrated under vacuum yielding a sticky white solid which was subjected to the next step without further purification (3.41 g, 9.70 mmol; 73%). ¹H NMR (300 MHz, CDCl₃): δ 0.88 (t, 3H), 1.24-1.33 (m, 38H), 1.55 (m, 2H), 3.26 (t, 2H).

docosan-1-amine:³



1-Azidodocosane (3.41 g, 9.72 mmol) was dissolved in hexane (52 mL), followed by addition of 10% Pd/C (0.18 g). The mixture was shaken and hydrogenated at 62 psi at RT for 3 hours. After gravity filtration through Celite on a coarse glass frit, the filtrate was concentrated to give a white solid which was recrystallized from EtOAc to give the final white powder (2.45 g, 7.52 mmol; 77%). m.p. 64-66 °C; R_f 0.10 (98/2 CHCl₃/MeOH); ¹H NMR (300 MHz, CDCl₃): δ 0.88 (t, 3H), 1.20-1.35 (m, 40H; 2H), 1.44 (m, 2H), 2.68 (t, 2H). m.p. 64-66 °C. MS (LC-MSD-Tof): m/z: 326.4 [M+H]⁺ calcd [M+H]⁺: 326.38.

4,6-di(docosylamino)-*m*-quinone (**C22m**)



4,6-Diaminoresorcinol dihydrochloride (0.10 g, 0.48 mmol) was dissolved in ethanol (16 mL). Docosan-1-amine (1.18 g, 3.63 mmol) was added to the reaction mixture to give a dark pink solution. The solution changed to dark brown/green with time. The mixture was left to stir for 7 hours, and then was left on ice for 15 min. The solid was collected by vacuum filtration, washed with cold ethanol and air dried. The crude product was dissolved in a minimal amount of chloroform, purified using centrifugal chromatography, 98:2 CHCl₃/MeOH, on silica and dried under vacuum to yield the final product (253.8 mg, 0.34 mmol; 70.8%). The dissolved form of **C22m** is red, while the powder form is green. m.p. 92-93 °C; *R_f* 0.37 (98:2 CHCl₃/MeOH); ¹H NMR (500 MHz, CDCl₃) δ 0.88 (t, 6H, CH₃), 1.34 (m, 76H, CH₂-CH₂-CH₂), 1.75 (q, 4H, NH-CH₂-CH₂), 3.36 (p, 4H, NH-CH₂), 5.13 (s, 1H, NH-C-CH), 5.47 (s, 1H, O-C-CH), 8.21 (br s, 2H, NH); ¹³C (125 MHz, CDCl₃) δ 14.08 (CH₃), 22.66, 26.91, 28.29, 29.14, 29.33, 29.40, 29.53, 29.60, 29.64, 29.68, 31.90, 43.28, 80.48(N-C-C), 98.76(O-C-C), 156.71(N-C), 172.25 (O-C). MS (LC-MSD-Tof): m/z: 755.7 [M+H]⁺ calcd [M+H]⁺: 755.74.

Section 3. Double deck packing at chemisorbed interfaces

Although, we are the first to introduce the idea of the double deck packing of alkyl chain at *physisorbed* interface, at *chemisorbed* interfaces, similar double-deck packing has already been proposed.^[2-13] For the SAM δ phase besides the well known ‘standing up’ phase (φ) of alkanethiol SAMs at higher coverage, there is a stacked-lying down phase (δ) and an unstacked-lying down phase (β) existing at intermediate and low surface coverage, respectively. From high-resolution STM images, the number of alkyl chains appears to be half as expected for the stacked-lying down phase (δ).^[10] Soththewes *et al.* found the depth of the troughs to be about twice the height for the β phase in comparison to the δ phase.^[12] Wu *et al.* studied the dynamics of decanethiol self-assembled monolayers on Au and discovered that the δ phase has much lower dynamics than the β phase. They believe that the alkyl chains in the δ phase experience an even larger van der Waals interaction as compared to the alkyl chains in the β phase.^[13] Furthermore, a direct observation of stacked alkyl chains has been reported using

UHV-STM.^[11] All evidence is consistent with these proposed double-deck structural models. Zeng *et al.* have even made use of these striped alkanethiol structures to immobilize C₆₀. They found that C₆₀ preferably adsorbed on the δ phase as opposed to the β phase stating that, ‘the furrow created by the stacked packing of alkyl chains stabilized C₆₀’.^[6] From multiple evidence: (i) direct STM visualization (Figure 7) and (ii) multilayer growth (Figure 9) and parallel evidence in chemisorbed systems, we proposed double-deck packing with unaccounted alkyl chains overlaying on top other alkyl chains as an alternative to the ‘flying alkyl chain model’.

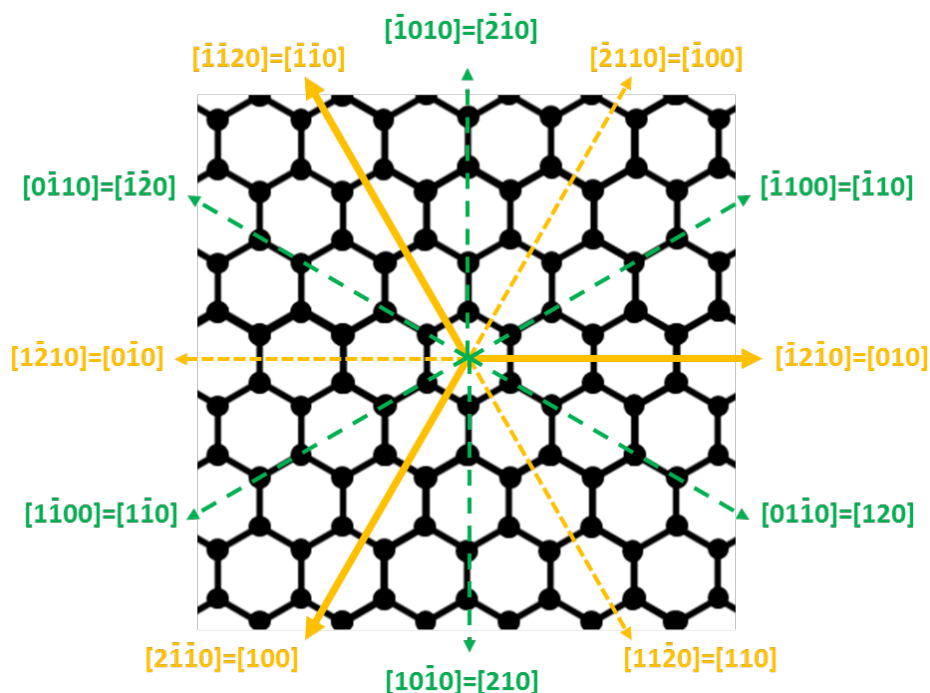


Figure S1. Symmetry axes of graphite. The main symmetry axes are colored in orange. The sub axes are colored in green. The normals are indicated in blue.

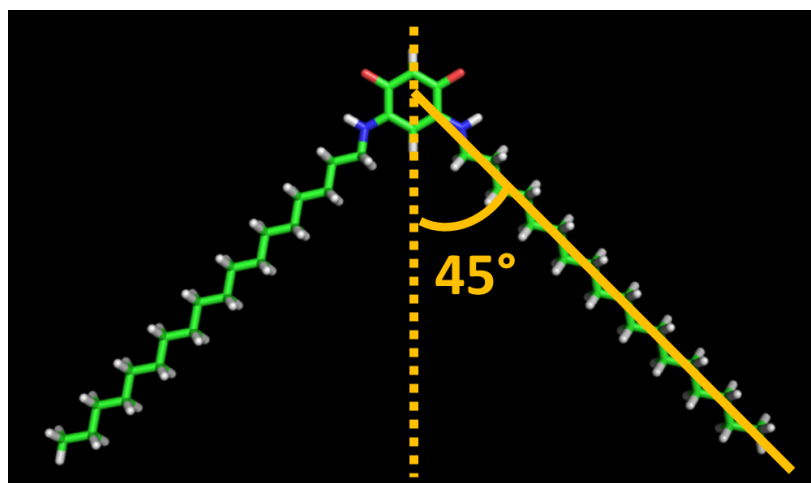


Figure S2. MM optimized **C18m** in vacuum showing that alkyl chains prefer to open like V shape.

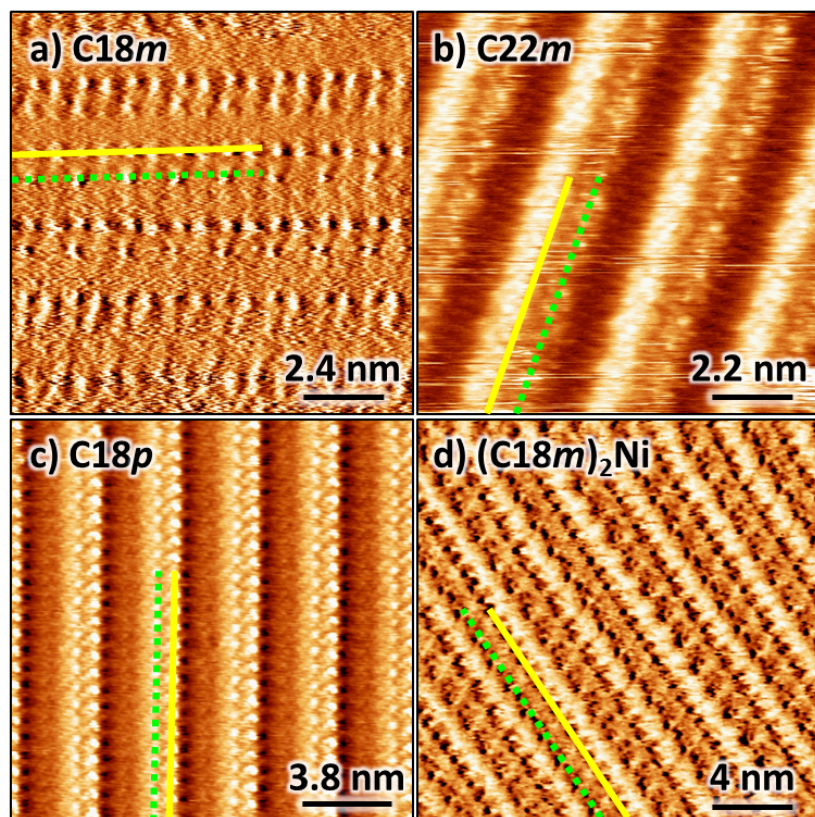


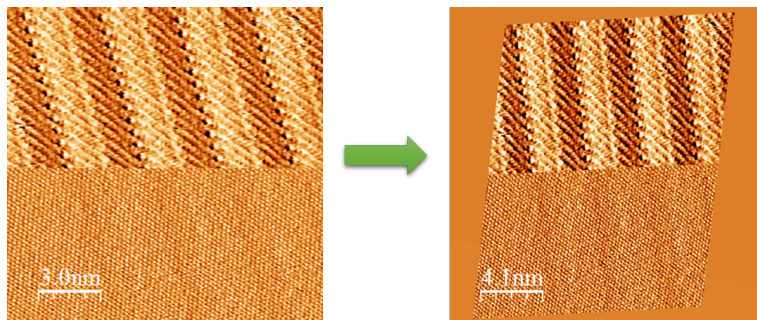
Figure S3. Evidence for parallel double layer formation. The yellow solid lines and green dotted lines indicate head-group rows from two different layers. a) $I_t = 13$ pA, $V_b = -650$ mV. b) $I_t = 20$ pA, $V_b = 580$ mV. c) $I_t = 18$ pA, $V_b = 550$ mV. d) $I_t = 25$ pA, $V_b = -1450$ mV.

Section 4: How to calibrate an STM image using WSxM 5.0

Proper calibration of STM images can never be stressed enough. Here a detailed tutorial about STM image calibration using WSxM is prepared for new STM user. WSxM, a free software, works similar to the commercially available SPIP software. WSxM can be conveniently downloaded from the WSxM official website.^[14]

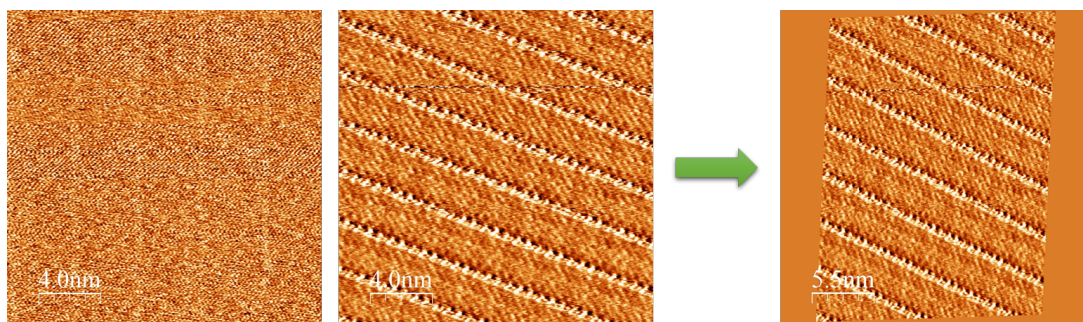
Two calibration methods are explained in this tutorial:

Method I:



Using one half-half image (or split image) – Imaging self-assembled monolayer (SAM) to midway followed by immediately changing the voltage to view the underlying graphite substrate. More reliable results are obtained after the instrument has been stabilized/equilibrated by repeating several scans in the same area.

Method II:



Requirement: 1) One SAM image, 2) one HOPG image

In this case, it is highly recommended for both images to have the same dimension, scan direction (both scan up or both scan down) and both images should be sequential.

N.B. calibration steps that are identical with those in the method are not repeated to save space.

Method I:

Step 1: The process is started by first **opening an STM image file (Figure S4.1):** 

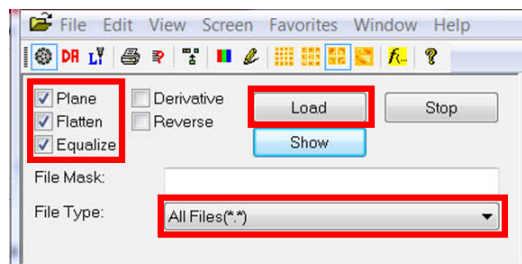


Figure S4.1. File opening window

In the above menu, check on **Plane Flatten** and **Equalize**, so that all the images that are opened will be automatically pre-processed. Choose the correct file type, select a file and load.


N.B.: Depending on the file format, a message may appear asking if you would like to extract the files. Click on **load**.

Tips: Images can be **dragged** into the program. If the **Plane, Flatten** and **Equalize** was preselected, any image dragged into the program will be processed as well.

The opened file should look like Figure S4.2.



Figure S4.2. Half-half image. STM current image of **C18p** at the TCB/HOPG interface. The bias voltage was changed during scanning, revealing atomic resolution of the HOPG. $15 \text{ nm} \times 15 \text{ nm}$; $I_t = 18 \text{ pA}$. $V_b = -350 \text{ mV}$ (SAM). $I_t = 18 \text{ pA}$, $V_b = 40 \text{ mV}$ (HOPG).

Step2: 2D Fast Fourier transform the image: 2D FFT 

2D FFT helps to find the repeating pattern in an image.

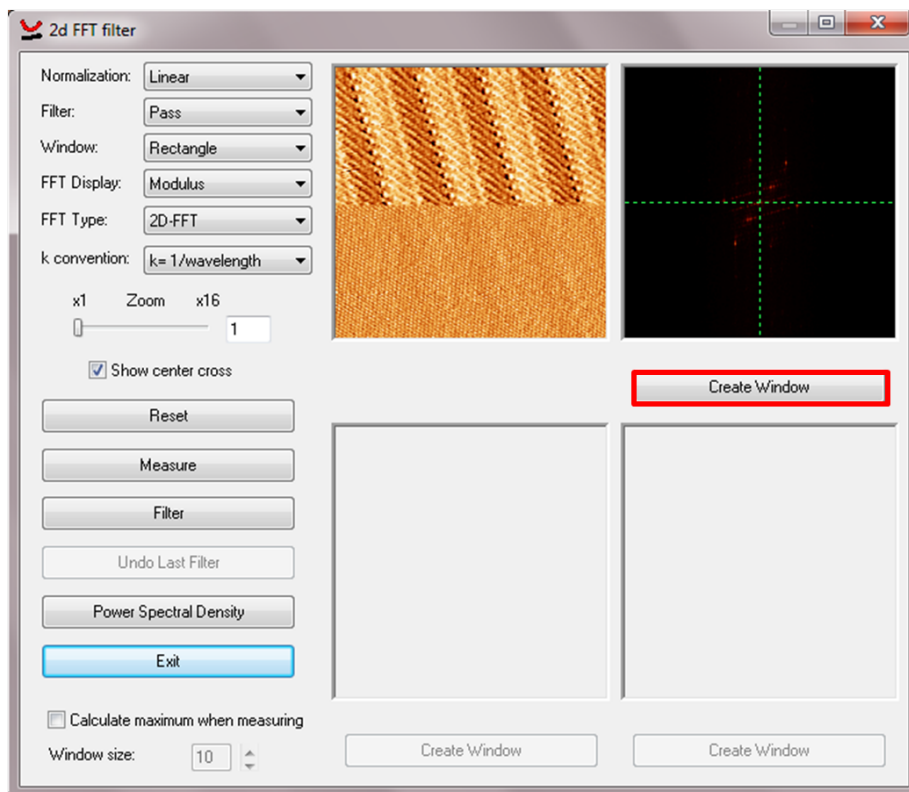


Figure S4.3. 2D FFT filter window for the half-half image.

In the above menu (Figure S4.3), click on **Create Window**.

A 2D FFT image of the half-half image will open in a new window. The 6 outer spots showing the symmetry or repeating pattern of HOPG, while the inner pattern decodes the repeating pattern(s) within the SAM.

Step 3: Zoom in: 

Press Shift (to get a square selection tool) and hold the left mouse key to select a region of interest. The zoomed in figure should look like Figure S4.4.

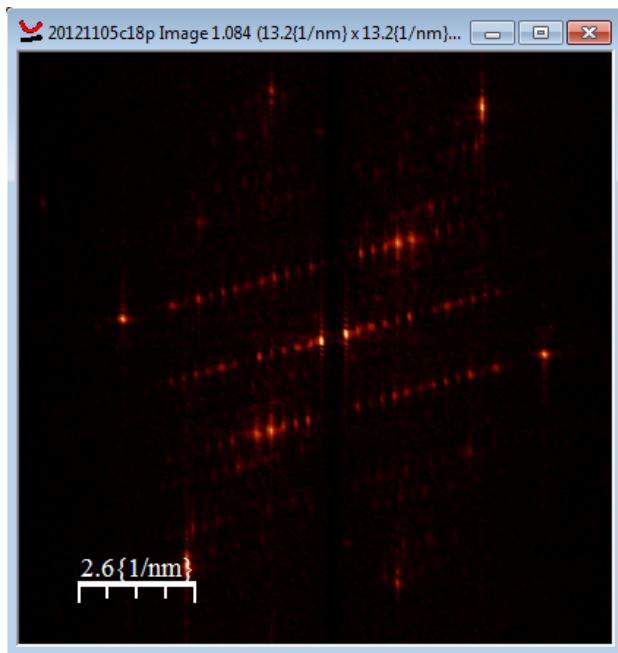


Figure S4.4. Enlarged 2D FFT image

Step 4: Rotate 90°: 

Using the rotation menu (Figure S4.5).

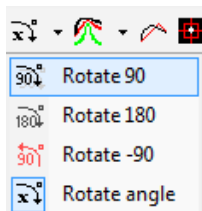




Figure S4.5. Rotation angle menu

Step 5: Redimension the image: 

Due to the cropping, the zoomed in image has lower resolution (number of lines). It is necessary to redimension the image to have the same resolution as the original image for the next calibration step (N.B. a typical STM image has a resolution of 512×512 points).

To verify the resolution of an image: 1) select the image with a single left click and 2) open the redimension window . The image resolution can be found in the Redimension window (Figure S4.6 beside Actual rows/columns number). Type 512 in both red highlighted boxes to redimension the image.

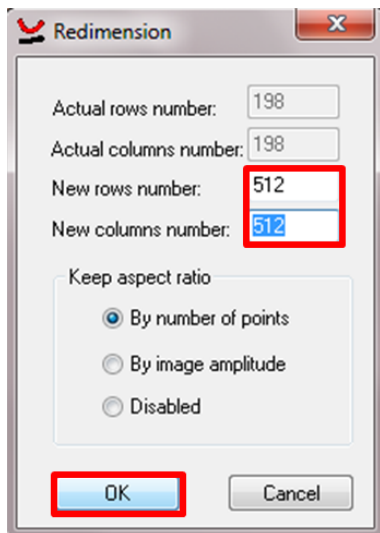


Figure S4.6. Redimension window

Step 6: Multiple lattice using the **Lattice menu** (Figure S4.9):

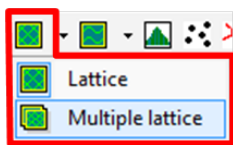


Figure S4.7. Lattice menu

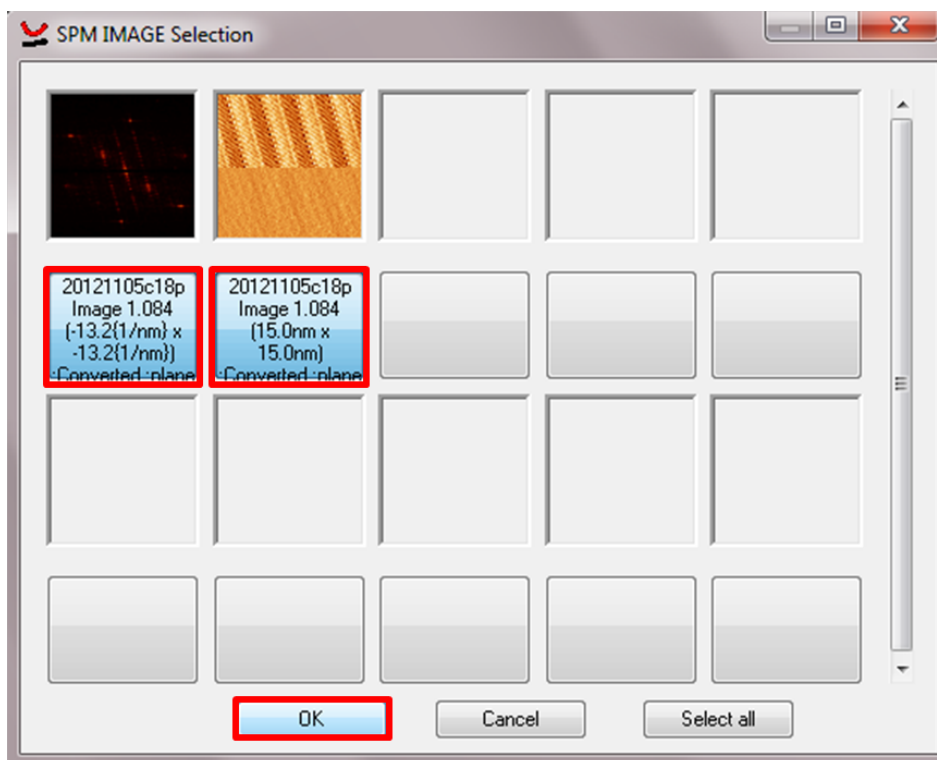


Figure S4.8. Multiple lattice Image Selection window.

In the resulting **Multiple lattice Image Selection** window (Figure S4.8), more images (with the same resolution) would show up if they are opened in the WSxM software. For the purpose of calibration, select the real space image and click on OK to obtain the lattice correction window (Figure S4.9).

Notice in the above example, the FFT image should appear on the most left, before the real space image. If not, cancel the selection, and select the FFT image with a single left click and

re-open the **Multiple lattice Image Selection** window .

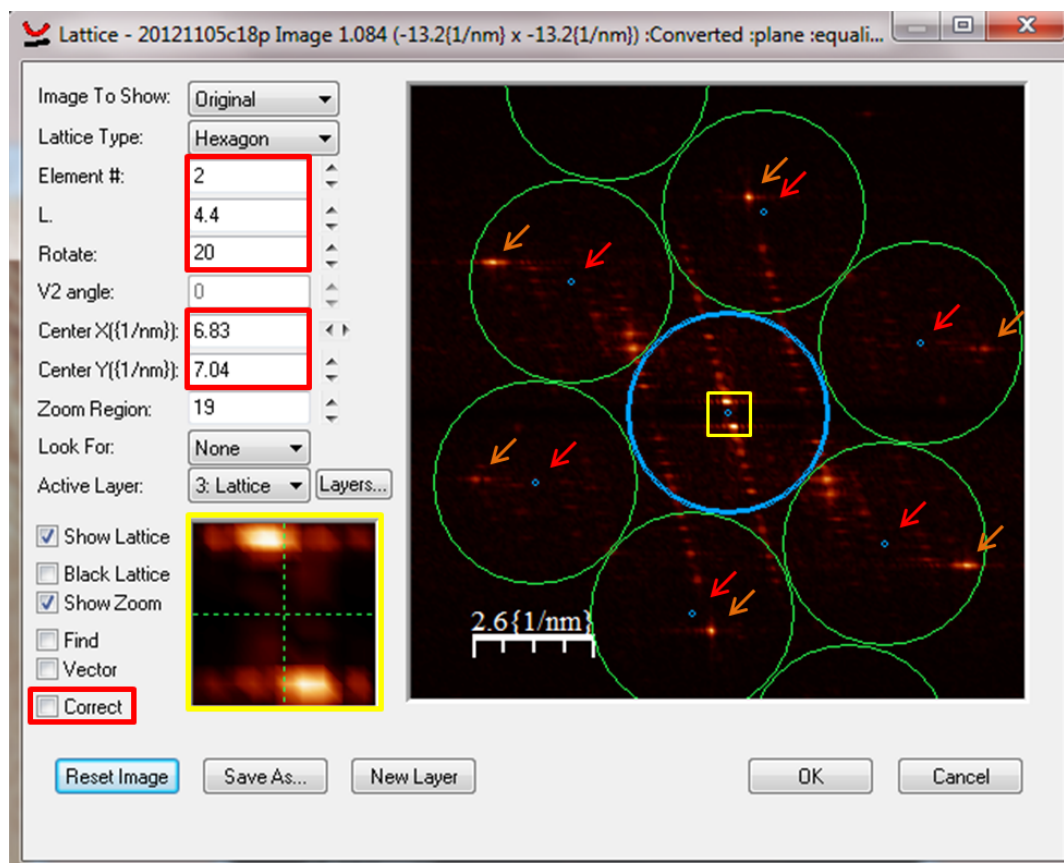


Figure S4.9. Lattice correction window

In the lattice correction window (Figure S4.9), center the blue circle using the zoomed-in image on the left (highlighted with a yellow square). Adjust the size of the green circles by changing the 'L' parameter. Note that the distance from the center of the blue circle to the centers of the green circles, highlighted with red arrows, should be shorter than the distance to the six HOPG orange spots, highlighted with orange arrows, to prevent cropping of the real space image) Rotate the position of green circles by changing 'rotate' parameter, so that they are as close to the orange spots as possible. Check the **Correct** box.

Click on one of the six HOPG bright orange spots followed by clicking on the nearest blue spot. Repeat this for the remaining five HOPG spots. **Right click** the mouse to end the correction. (The procedure can be repeated by clicking on **Correct** box again or one can start over by clicking on **Reset Image**)

After correction, Ok all the way out. The corrected SAM image will appear as shown in Figure S4.10.

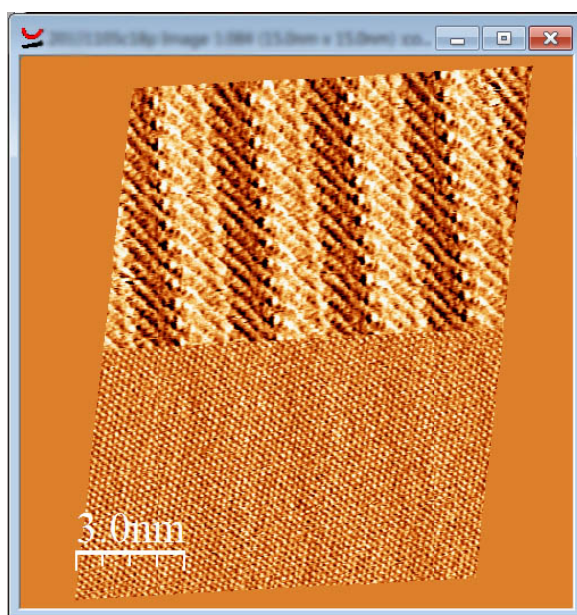


Figure S4.10. Lattice corrected half-half image

Step 7. Size calibration

At this point, the lattice shape of the image has been corrected. The next step is to correct the lattice size.

Click on  to zoom into the HOPG region (Figure S4.11)

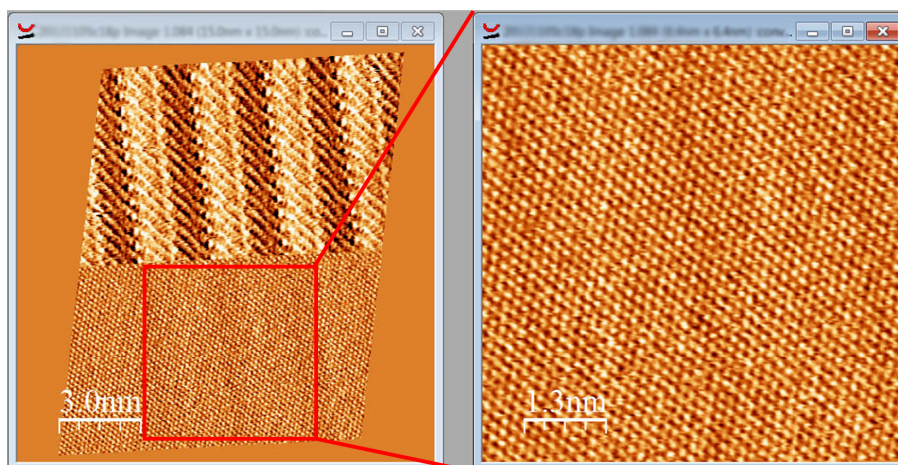



Figure S4.11. Zoomed in HOPG image

Get a 2D FFT image of the HOPG by click 

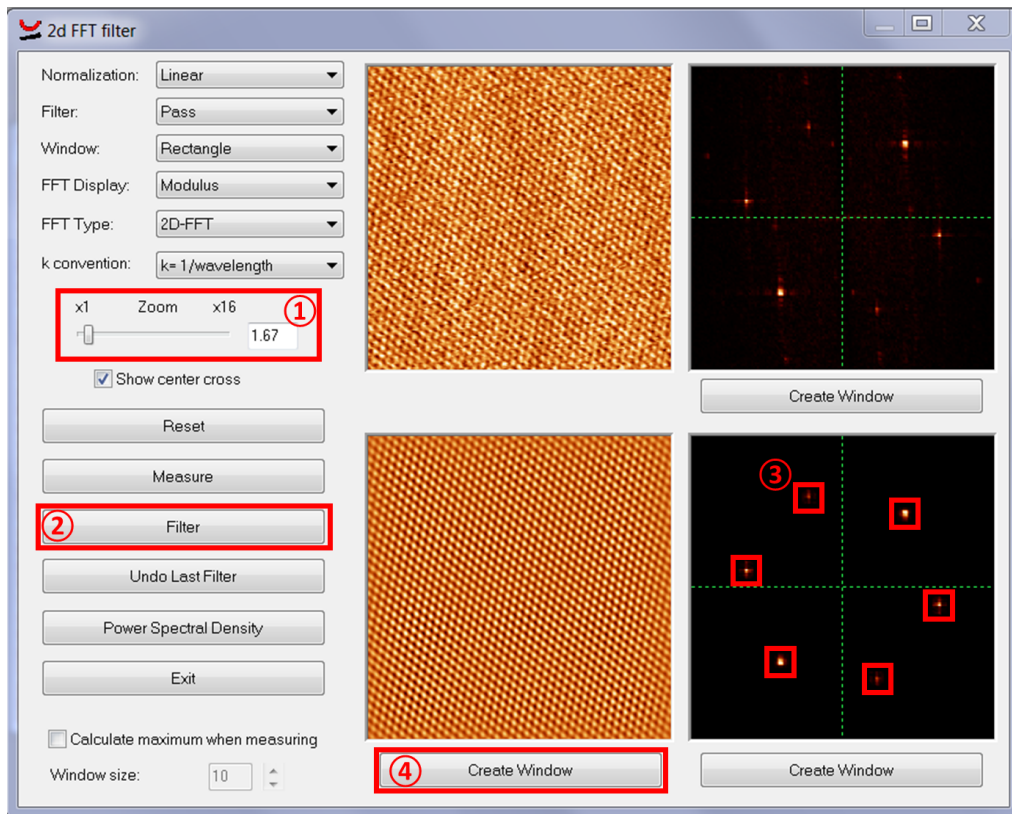






Figure S4.12. 2D FFT window for HOPG

First slightly increase the size of the HOPG FFT dots by the **Zoom** bottom on the left of the window. Second, left click the **Filter** bottom. Third, drag boxes around the HOPG FFT dots (Figure S4.12, step 3), followed by a right click. By doing so, image noise is removed and one can visualize the HOPG pattern more clearly. Finally, click on **Create Window**.

Measure the distance between two HOPG spots:  

Make a line profile parallel to one of the axes of HOPG using . Left click the Profile image, then click  and place the two square boxes directly on top of the two HOPG peaks (Figure S4.13 right) to get distance measurement. The distance can be found in the information bar at the bottom of the main window. To increase the measurement accuracy, it is better to get an averaged measurement. For example in Figure S4.13, the distance between 26 spots is 4.56nm, so the separation of two HOPG equals to $4.56/26=0.17538$ nm.

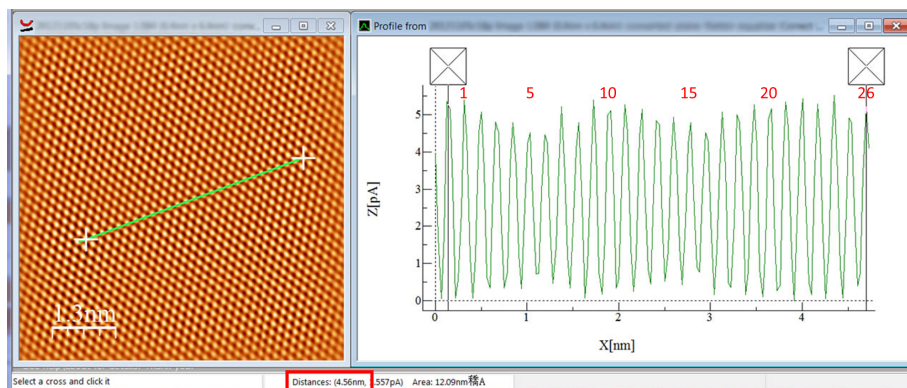




Figure S4.13. Left) 2D FFT filtered HOPG image, and right) corresponding line profile

Resize the image:  

The distance of 0.17538 nm should be calibrated to the standard HOPG distance which is 0.246 nm. To do so, first calculate the ratio between actual distance and standard distance.

$$\text{Ratio} = \frac{0.246}{0.17538} = \mathbf{1.4027}$$

Click on  to open Recalibrate window. Type 1.4027 into **Factor** box (Figure S4.14). Select **Square Pixels** (i.e. the y-axis will be multiplied by the same factor as the x-axis). After clicking on OK, a fully calibrated half-half image will look like Figure S4.15.

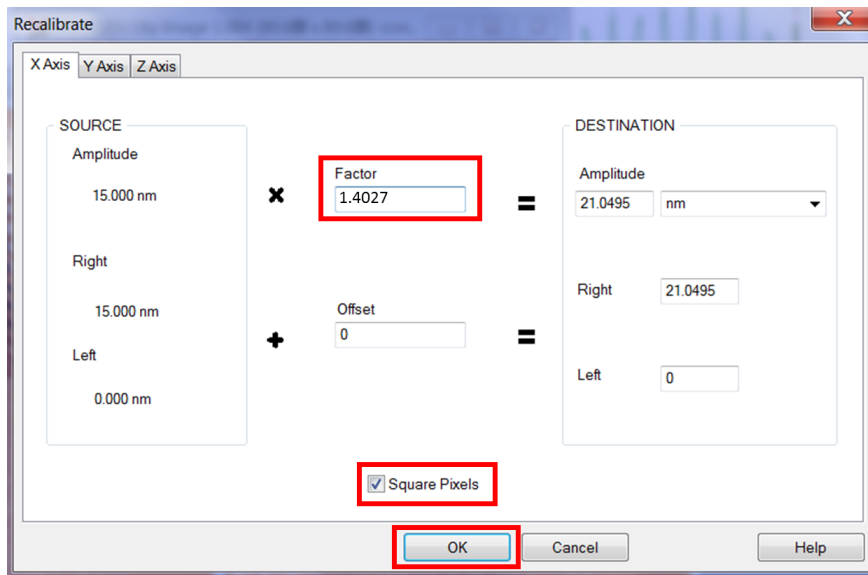


Figure S4.14. Recalibrate window

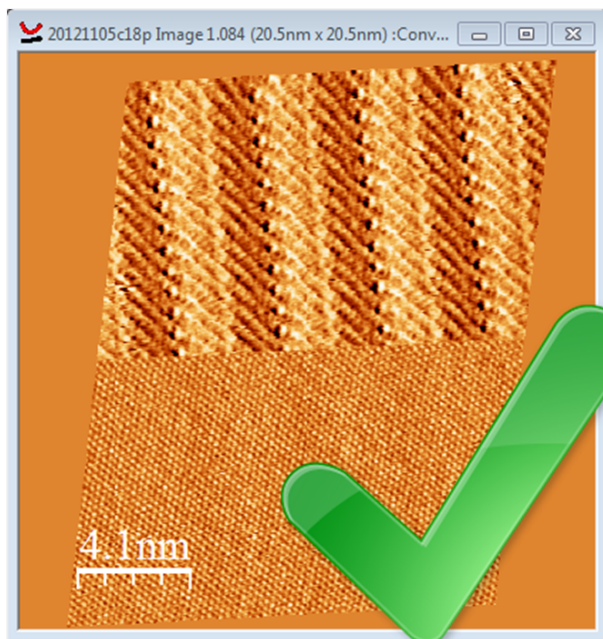


Figure S4.15. Fully calibrated half-half image.

Method two:

The procedures of method two are very similar to method one. An illustrated procedure of method two is described below. (N.B. refer to method one for detailed repeated steps).

Step 1: Open one HOPG image and one SAM image: 

The opened files will look like Figure S4.19.

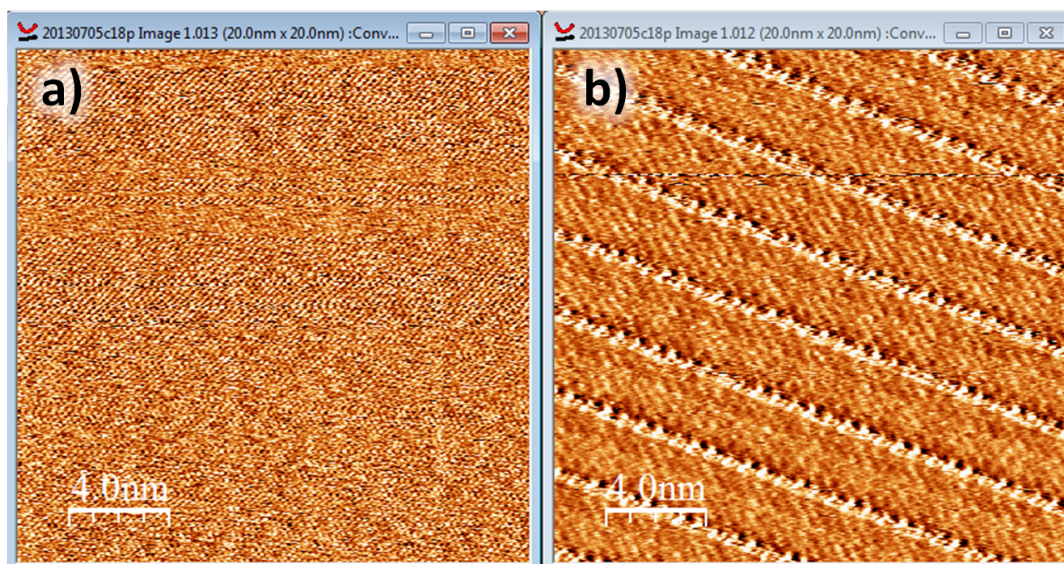


Figure S4.16. a) HOPG image $20 \text{ nm} \times 20 \text{ nm}$; $I_t = 18 \text{ pA}$. $V_b = 41 \text{ mV}$. b) STM current image of C18p at the TCB/HOPG interface. $20 \text{ nm} \times 20 \text{ nm}$; $I_t = 18 \text{ pA}$. $V_b = -300 \text{ mV}$.

Step 2: 2D Fast Fourier transform the HOPG image: 2D FFT 

Only 2D FFT the HOPG image, not the SAM image. The 2D FFT image of HOPG should contain 6 bright spots (Figure S4.20).

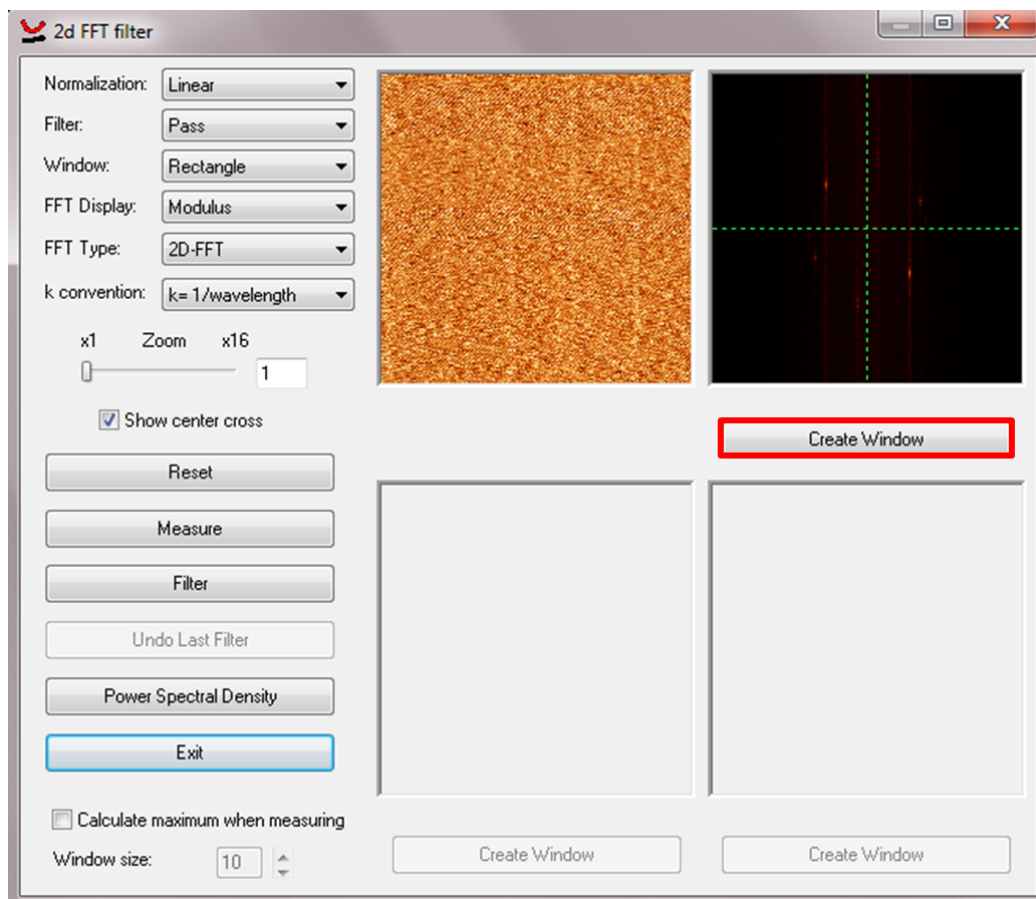



Figure S4.17. 2D FFT filter window for HOPG image

Step 3: Zoom in: 

Press Shift to draw a square, by holding left mouse key, which just fit the six HOPG spots. More detail see Method One.

Step 4: Rotate 90°: 

More detail see Method One.

Step 5: Redimension the image: 

If the original image is 512×512 by points, redimension the zoomed in image to the same resolution. More detail see Method One.

Step 6: Multiple lattice: 

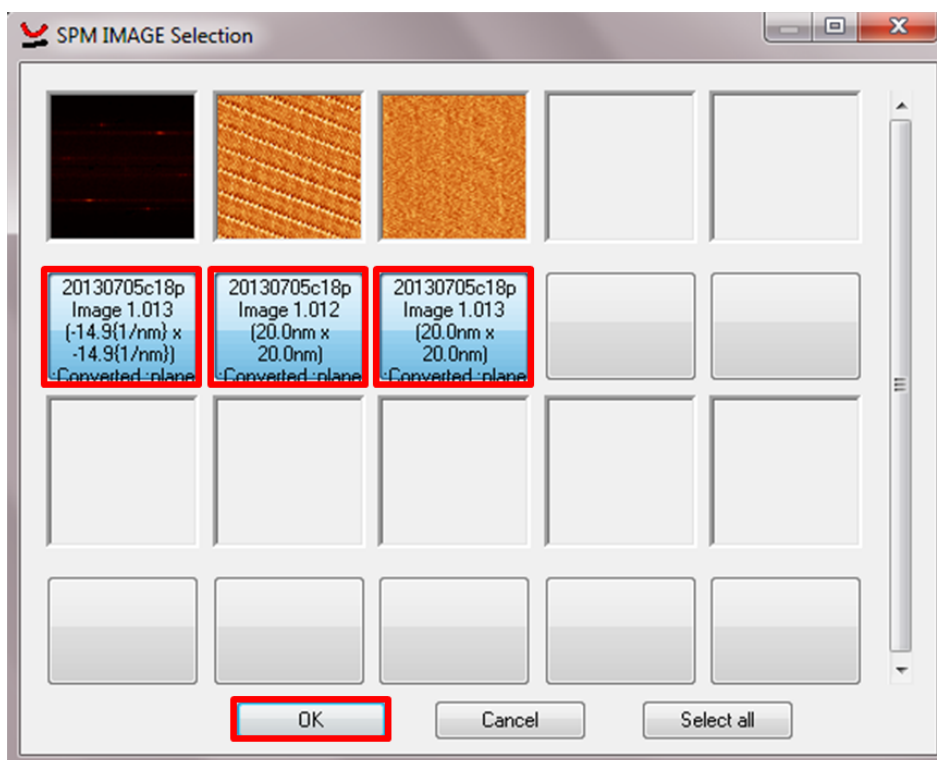


Figure S4.18. Multiple lattice image selection window

The 2D FFT image of HOPG should appear in the first image window (Figure S4.22). Select both the SAM image and the HOPG image.

Calibrate the shape of the six HOPG spots as described in step 6 of method one. And continue rest of the calibration following the Method One.

One now can finally extract **unit cell perimeters, β angle and the domain rotation with respect to underlying substrate** from this fully calibrated image. One can then use properly measured unit cell perimeters to calibrate images that do not have HOPG references.

References

- [1] Y. Fang, N. Salame, S. Woo, D. S. Bohle, T. Friscic, L. A. Cuccia, *CrystEngComm* **2014**, *16*, 7180-7185.
- [2] G. E. Poirier, *Langmuir* **1999**, *15*, 1167-1175.
- [3] G. E. Poirier, T. M. Herne, C. C. Miller, M. J. Tarlov, *J. Am. Chem. Soc.* **1999**, *121*, 9703-9711.
- [4] M. Toerker, R. Staub, T. Fritz, T. Schmitz-Hubsch, F. Sellam, K. Leo, *Surf. Sci.* **2000**, *445*, 100-108.
- [5] G. E. Poirier, W. P. Fitts, J. M. White, *Langmuir* **2001**, *17*, 1176-1183.
- [6] C. G. Zeng, B. Wang, B. Li, H. Q. Wang, J. G. Hou, *Appl. Phys. Lett.* **2001**, *79*, 1685-1687.

- [7] M. Epple, A. M. Bittner, A. Kuhnke, K. Kern, W. Q. Zheng, A. Tadjeddine, *Langmuir* **2002**, *18*, 773-784.
- [8] W. P. Fitts, J. M. White, G. E. Poirier, *Langmuir* **2002**, *18*, 2096-2102.
- [9] M. Godin, P. J. Williams, V. Tabard-Cossa, O. Laroche, L. Y. Beaulieu, R. B. Lennox, P. Grütter, *Langmuir* **2004**, *20*, 7090-7096.
- [10] S. S. Li, L. P. Xu, L. J. Wan, S. T. Wang, L. Jiang, *J. Phys. Chem. B* **2006**, *110*, 1794-1799.
- [11] O. Voznyy, J. J. Dubowski, J. T. Yates, P. Maksymovych, *J. Am. Chem. Soc.* **2009**, *131*, 12989-12993.
- [12] K. Sotthewes, H. Wu, A. Kumar, G. J. Vancso, P. M. Schon, H. J. W. Zandvliet, *Langmuir* **2013**, *29*, 3662-3667.
- [13] H. Wu, K. Sotthewes, A. Kumar, G. J. Vancso, P. M. Schon, H. J. W. Zandvliet, *Langmuir* **2013**, *29*, 2250-2257.
- [14] I. Horcas, R. Fernández, J. M. Gómez-Rodríguez, J. Colchero, J. Gómez-Herrero, A. M. Baro, *Rev. Sci. Instrum.* **2007**, *78*, 013705.